Code synchronization based on lumped time-delay compensation scheme with a linearly chirped fiber Bragg grating in all-optical analog-to-digital conversion*

Wang Tao(王 涛)[a)†], Kang Zhe(康 哲)[a)], Yuan Jin-Hui(苑金辉)[a)b)], Tian Ye(田 野)[a)], Yan Bin-Bin(颜玢玢)[a)], Sang Xin-Zhu(桑新柱)[a)], and Yu Chong-Xiu(余重秀)[a)]

[a)] *State Key Laboratory of Information Photonics and Optical Communications (Beijing University of Posts and Telecommunications), Beijing* 100876 *China*

[b)] *Laboratory of Nanophotonic Functional Materials and Devices, South China Normal University, Guangzhou* 510006, *China*

(Received 18 December 2013; revised manuscript received 21 March 2014; published online 10 August 2014)

We propose a novel lumped time-delay compensation scheme for all-optical analog-to-digital conversion based on soliton self-frequency shift and optical interconnection techniques. A linearly chirped fiber Bragg grating is optimally designed and used to compensate for the entire time-delays of the quantized pulses precisely. Simulation results show that the compensated coding pulses are well synchronized with a time difference less than 3.3 ps, which can support a maximum sampling rate of 151.52 GSa/s. The proposed scheme can efficiently reduce the structure complexity and cost of all-optical analog-to-digital conversion compared to the previous schemes with multiple optical time-delay lines.

Keywords: all-optical analog-to-digital, lumped time-delay compensation, soliton self-frequency shift, linearly chirped fiber Bragg grating

PACS: 42.65.Re, 42.65.Tg, 42.79.Dj, 42.81.Dp **DOI:** 10.1088/1674-1056/23/10/104212

1. Introduction

Analog-to-digital conversion (ADC) has been studied as an important technology in many electronic or photonic systems to digitize the analog electric signals. In recent years, tremendous development of the ultra-wide-bandwidth applications requires ADC with ultrafast sampling and high resolution performances. Although significant progress of electrical circuit technology has realized the high-resolution ADC whose resolution is ten or more bits at moderate sampling rate ranging from megasamples per second (MS/s) to gigasamples per second (GSa/s), there is an unavoidable tradeoff between the sampling rate and the resolution bit due to the electrical jitter of the sampling aperture and ambiguity of the comparators.[1–3] All-optical ADC (AOADC) with entire optical approaches to the sampling, quantizing, and coding block can provide many advantages over the electrical counterparts.[2,3] The most significant advantage of AOADC for sampling is to reduce the jitter of sampling aperture by using a ultra-stable mode-locked laser source.[4] The previous optical quantization schemes include utilizing cross-phase modulation (XPM) effect,[5] soliton self-frequency shift (SSFS) effect,[6,7] higher order soliton fission,[8] slicing the spectrum of supercontinuum (SC),[9,10] and self-phase modulation (SPM) effect of Gaussian pulse in optical fiber.[11] Among these shcemes, optical quantization using SSFS effect is a promising candidate since it has ultrafast response speed and is transparent for sampling rate. Several outstanding results on SSFS-based ADCs have been obtained.[6,12–16] However, time-delays between different quantized pulses occur simultaneously in the SSFS process. The time-delay problem can directly induce the non-synchronization of the coding pulse trains and result in the coding error. Time-delay compensation method with multiple optical time-delay lines (TDLs) is proposed in previous schemes.[12–16] This method is complicated and costly, especially in the case of high quantization resolution.

In this paper, we propose a novel lumped time-delay compensation scheme for the synchronization of coding. By optimally designing a linearly chirped fiber Bragg grating (LCFBG) rather than multiple TDLs, the time-delays of quantized pulses can be compensated for precisely. The numerical analysis is simulated and discussed.

*Project supported by the National Basic Research Program, China (Grant Nos. 2010CB327605 and 2010CB328300), the National High-Technology Research and Development Program of China (Grant No. 2013AA031501), the National Natural Science Foundation of China (Grant No. 61307109), the Specialized Research Fund for the Doctoral Program of Higher Education of China (Grant No. 20120005120021), the Fundamental Research Funds for the Central Universities, China (Grant No. 2013RC1202), the Program for New Century Excellent Talents in University, China (Grant No. NECT-11-0596), the Beijing Nova Program, China (Grant No. 2011066), the Fund of State Key Laboratory of Information Photonics and Optical Communications (Beijing University of Posts and Telecommunications), China, the China Postdoctoral Science Foundation (Grant No. 2012M511826), and the Postdoctoral Science Foundation of Guangdong Province, China (Grant No. 244331).

†Corresponding author. E-mail: wangtaoseasky@163.com

© 2014 Chinese Physical Society and IOP Publishing Ltd

2. Principles and schematic design

The schematic diagram of an all-optical ADC with 3-bit quantization resolution is shown in Fig. 1. It consists of two parts: optical quantization based on SSFS in highly nonlinear fiber (HNLF) and optical coding based on a topology structure of the binary coding.

As shown in Fig. 1, the analog-sampled signals propagate in an HNLF for the generation of SSFS to realize power-to-wavelength conversion. After the HNLF, the central wavelength of each analog-sampled signal has a red shift.[17] The amount of the central wavelength shift is in direct proportion to peak power of signal. So we can distinguish different powers of analog-sampled signal by referring to the change of central wavelength. And different time-delays of quantized pulses occur simultaneously in time domain. Here we can realize optical quantization by SSFS effect. To separate the signals of different central wavelengths, we use a dispersion device-like arrayed waveguide grating (AWG). By setting the parameters of AWG, signals of different powers occur at specific ports of AWG and then be sent to coding module. In coding module, the optical interconnection is realized by several couplers, TDLs, and photodiodes b_1, b_2, and b_3. The interconnection topology is based on a binary conversion table, which is shown in the upper left part of Fig. 1.

	b_1	b_2	b_3
a_0	0	0	0
a_1	1	0	0
a_2	0	1	0
a_3	1	1	0
a_4	0	0	1
a_5	1	0	1
a_6	0	1	1
a_7	1	1	1

$$b_1 = a_1 + a_3 + a_5 + a_7,$$
$$b_2 = a_2 + a_3 + a_7 + a_7,$$
$$b_3 = a_4 + a_5 + a_6 + a_7,$$

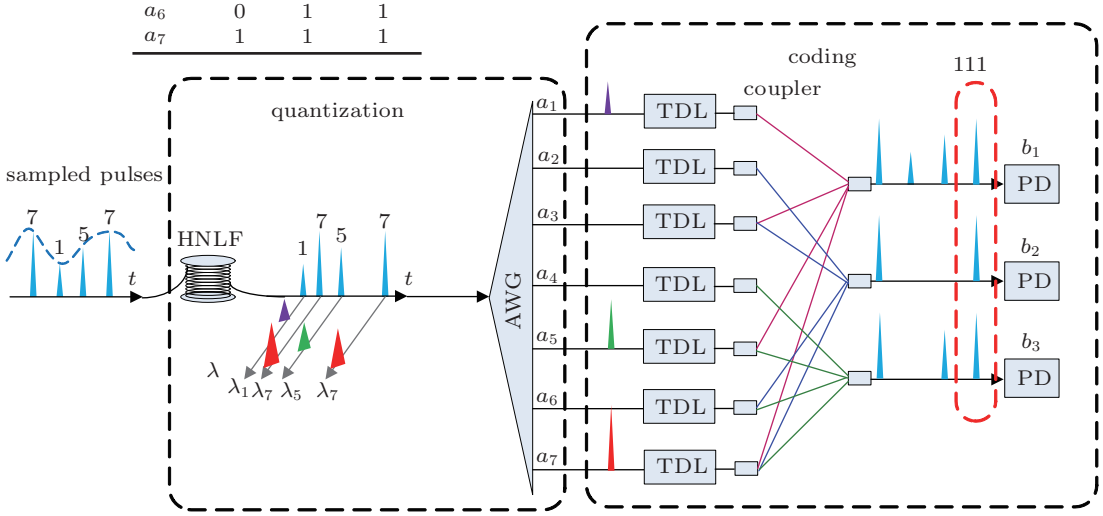


Fig. 1. (color online) Schematic diagram of the proposed optical quantization and coding scheme. HNLF: highly nonlinear fiber, AWG: arrayed waveguide grating, TDL: time delay lines, PD: photodiode.

The a_1–a_7 are quantized pulses and the outputs b_1–b_3 are binary signals in Table 1 which is shown in the upper right part of Fig. 1, where we can see the outputs b_1–b_3 are formed by a_1–a_7. In the outputs of photodiodes, analog-sampled signals are converted into 3-bit binary code.

The scheme utilizing SSFS effect has a problem that sampled pulses with different peak powers have different time-delays in the HNLF. The dynamic behavior of optical pulse through an optical fiber can be described by generalized nonlinear Schrödinger equation (GNLSE). Using the method of moment (MOM)[18] to solve the GNLSE semi-analytically, the variation of time-delay can be obtained as follows:

$$\Delta t \propto \beta_2 \cdot \Omega \cdot z \propto D \cdot z \cdot \lambda_{\text{shift}} = D \cdot z \cdot (\lambda_c - \lambda_0), \qquad (1)$$

where Δt is the time-delay of optical pulse in SSFS, z the transmission distance in fiber, β_2 the second-order dispersion coefficient, Ω the frequency shift of optical pulse, $D = -2\pi c\beta_2/\lambda^2$ the dispersion parameter of fiber, λ_c the central wavelength of optical pulse after HNLF, and λ_0 the input wavelength. Equation (1) shows that the time-delay Δt in SSFS is in direct proportion to λ_c when the dispersion parameter and the length of optical fiber are constant. The mechanism of the proposed lumped time-delay compensation is shown in Fig. 2.

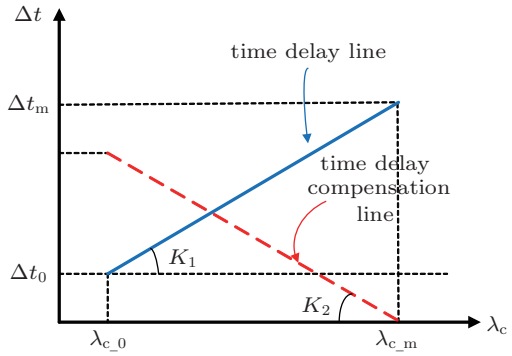


Fig. 2. (color online) Mechanism of the proposed lumped time-delay compensation.

Since the time-delay line is a straight line with the slope K_1, we can use a straight line with the slope of $K_2 = -K_1$ to compensate for the time-delay. The time-delay can be compensated for in different ways as long as the dashes line can be realized. The LCFBG has the characteristics to realize the time-delay compensation. When a wide bandwidth pulse is launched into an LCFBG, different wavelength components reflect at different positions. A simple variable method is utilized to study the influences of the several parameters on the bandwidth and time-delay.[19,20] The results show that the linear scope of time-delay line can be broadened and the ripple of the line can be reduced by increasing the total chirp coefficient and the length of LCFBG. Increasing the average variation of refractive index $\overline{\delta n_{\text{eff}}}$ is not useful to improve the linearity of time-delay line, but it is useful to broaden the reflection bandwidth. Apodization function $f(z)$ can reduce the side-lobe of reflectivity line and improve the linearity of time-delay line.[21,22] Based on the study results, we design the LCFBG and propose a lumped time-delay compensation scheme, as shown in Fig. 3. To obtain the output reflectivity R and time-delay Δt of LCFBG, the transmission matrix method[23] is used for simulation.

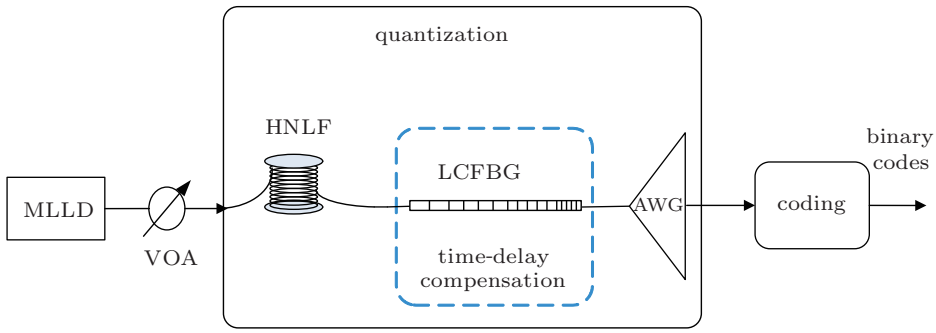


Fig. 3. (color online) Schematic diagram of the lumped time-delay compensation scheme with LCFBG. MLLD: Mode-locked laser diode, VOA: variable optical attenuator.

Comparing Fig. 3 with Fig. 1, the time-delay compensation is brought forward from coding module to quantization module. An LCFBG is inserted between the HNLF and AWG to compensate for the time-delay rather than several TDLs. The improvements are definitely useful for the integration and miniaturization of all-optical ADC.

3. Simulation and discussion

The dynamic behavior of the pulses in time and frequency domain during the quantization process is numerically analyzed by solving the GNLSE with split-step Fourier method, which gives more precise analytical solution than the MOM. In Fig. 3, the central wavelength of optical pulses generated by the mode-locked laser diode (MLLD) is 1558 nm. To simulate the sampled pulses with different peak powers, a variable optical attenuation (VOA) is used in Fig. 3 to generate the sampled pulses with different powers. For example, the peak powers Q_1, Q_2, Q_3, Q_4, Q_5, Q_6, and Q_7 of sampled pulses are 5.1 W, 7.0 W, 8.5 W, 10.0 W, 11.5 W, 13.0 W, and 15.0 W respectively. Q_0 with the peak power of 0 is of no use in the coding module, so it is neglected in our simulation. After transmitting in 1-km HNLF ($\gamma = 16\ \text{W}^{-1}/\text{km}$, $\alpha = 0.9$ dB/km, $D = +3$ ps/(nm/km)) for quantization, the central wavelengths of sampled pulses are shifted to specific positions. The spectral profiles of the optical pulses $Q_1 \sim Q_7$ after the HNLF are shown in Fig. 4.

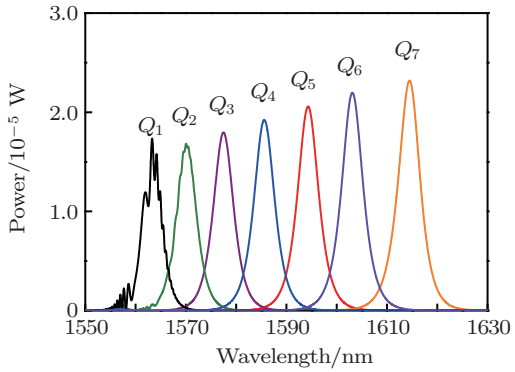


Fig. 4. (color online) Spectral profiles of the optical pulses $Q_1 \sim Q_7$ after the HNLF.

As shown in Fig. 4, the amount of central wavelength shift is in direct proportion to peak power of sampled signal. After passing through the HNLF, optical signals have been quantized. The signal whose peak power lies between the quantization levels will be quantified to the nearest quantization level.

The initial time interval of adjacent pulses is 25 ps since the sampling rate is 40 GSa/s as shown in Fig. 5(a). After the SSFS process, the pulses with different peak powers have different time-delays. The temporal profiles of the delayed pulses are shown in Fig. 5(b). The relationships between time-delay and input peak power with different values of dispersion D and length L of the HNLF are shown in Figs. 5(c) and 5(d) respectively. It is evident that the time-delay increases linearly as the input peak power of the pulse augments.

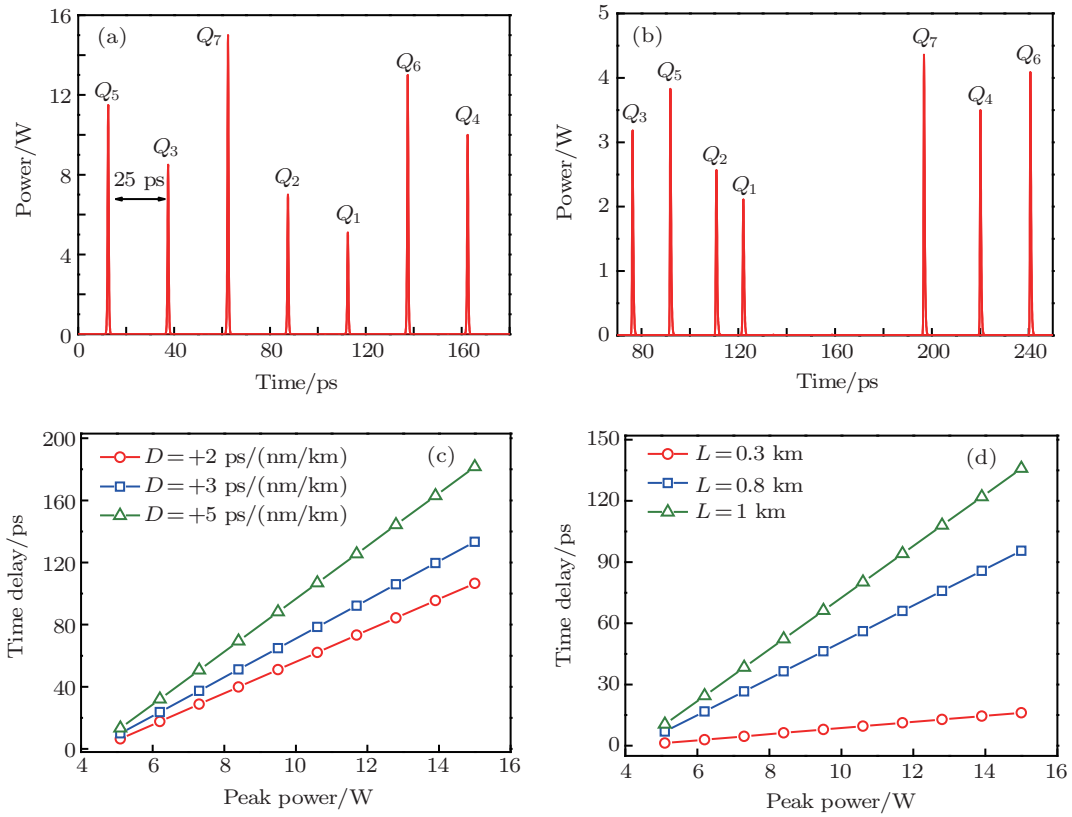


Fig. 5. (color online) Temporal profiles of the sampled pulses (a) before and (b) after passing through the HNLF, and the time-delays of quantized pulses as a function of input peak power with (c) different values of D and (d) different values of L.

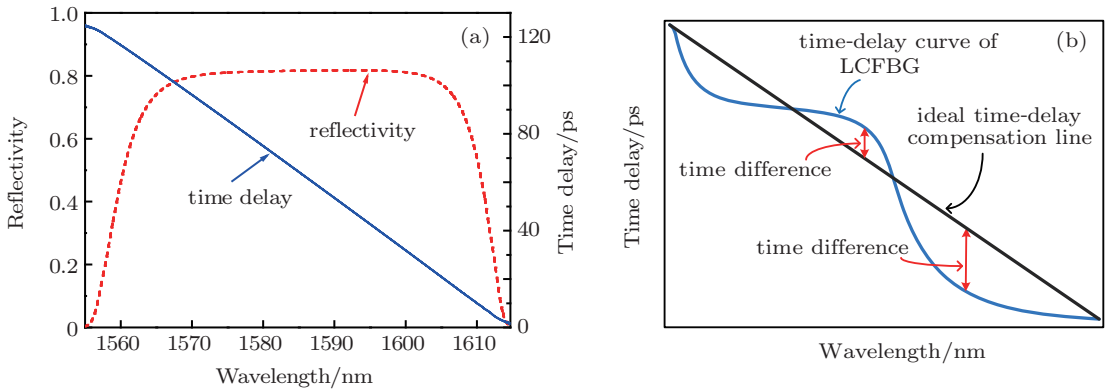


Fig. 6. (color online) (a) Plots of characteristics of LCFBG, and (b) illustration of the method for time difference calculation.

A comparison between Figs. 5(a) and 5(b) shows that the coding error will definitely occur without compensating for the time-delay in SSFS. Now an LCFBG is utilized to correct the error. In order to compensate for the time-delay accurately, length L_B and total chirp C of the LCFBG must be chosen carefully (when $\overline{\delta n_{\text{eff}}}$ and $f(z)$ are constant). After obtaining the time-delay compensation curves for different cases of L_B and C (for example, one curve is shown in Fig. 6(a)),

we compare them with the ideal time-delay compensation line to calculate the maximum time difference due to utilizing the method shown in Fig. 6(b), which is the detailed view of a small segment in Fig. 6(a). The calculated maximum time differences with the different values of L_B and C are shown in Fig. 7(a). The relationship between the bandwidth and the total chirp is shown in Fig. 7(b). The bandwidth of the LCFBG should cover the wavelength shift range of the SSFS effect to ensure that the time-delay of each quantized pulse can be compensated for. Since the minimum bandwidth in our scheme is 55 nm, the minimum total chirp is −55 nm.

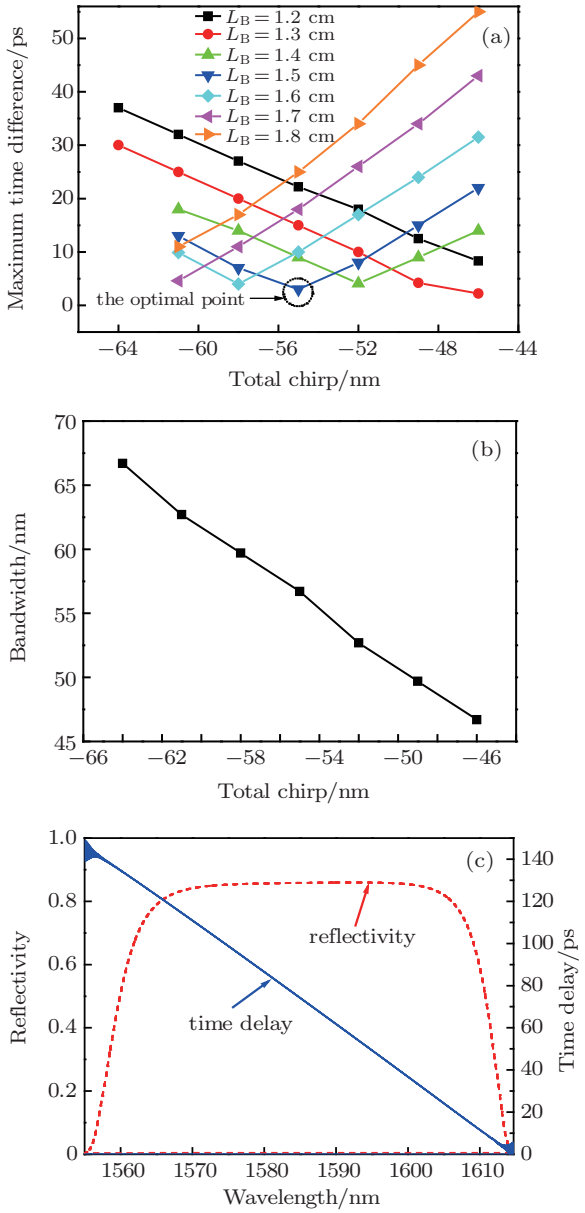


Fig. 7. (color online) (a) Calculated maximum time difference in the cases of different total chirps and lengths of the LCFBG, (b) the bandwidth as a function of the total chirp, and (c) the performances of the LCFBG with optimal parameters.

As shown in Fig. 7(a), the maximum time difference of 3.3 ps is obtained for the LCFBG with $L_B = 1.5$ cm and $C = -55$ nm. The corresponding optimal parameters of the LCFBG are $L_B = 1.5$ cm, $C = -55$ nm, $\overline{\delta n_{\text{eff}}} = 1.5 \times 10^{-3}$, $f(z) = \tanh(10z/L)\tanh[10(1 - z/L)]$. The performance of the optimal LCFBG is shown in Fig. 7(c), where the reflectivity bandwidth can reach 56 nm and the reflectivity is 0.8. The reflectivity curve shows very small ripples and the time-delay curve also has small ripples.

After the lumped time-delay compensation with LCFBG, the time interval of adjacent optical pulses is shown in Fig. 8. The maximum time interval is 28.00 ps while the minimum one is 22.05 ps. The coding results are shown in Fig. 9. The dashed lines are the judgment windows of the comparator. It is evident that the time-delays are accurately compensated for with the proposed scheme and no coding error occurs in the results.

The relationship between the supportable sampling rate S and the maximum time difference $\Delta\tau$ is shown in Eq. (2) and Fig. 10. It is evident that the supportable sampling rate decreases with the increase of the maximum time difference. Since the time difference is found to be no more than 3.3 ps, our proposed scheme can support the maximum sampling rate of 151.52 GSa/s.

$$S = \frac{1}{2\Delta\tau}. \tag{2}$$

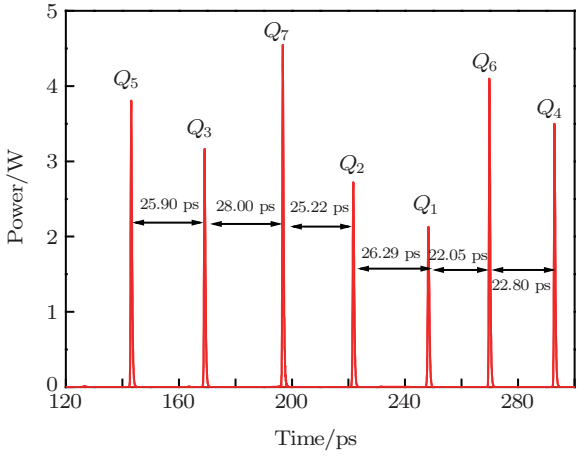


Fig. 8. (color online) Time intervals of adjacent optical pulses.

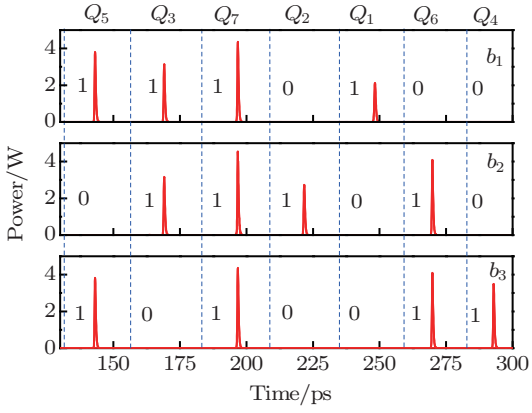


Fig. 9. (color online) Output temporal profiles of the three quantization channels and corresponding coding results.

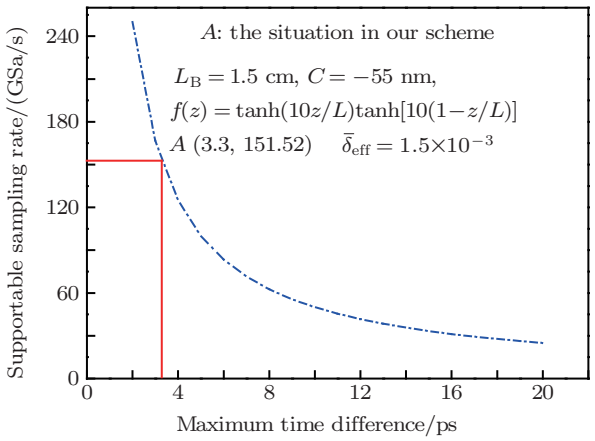


Fig. 10. (color online) Supportable sampling rate as a function of the maximum time difference.

4. Conclusion

In this paper, we proposed a novel lumped time-delay compensation scheme by utilizing an LCFBG in optical quantization for all-optical ADC. The linear relationship between the time-delay and the central wavelength position of the quantized pulse is analyzed. The simulation results show that the optimized LCFBG can compensate for the time-delay accurately with the time difference less than 3.3 ps. The proposed scheme can support a maximum sampling rate of 151.52 GSa/s with no coding error. Since the total wavelength range is 55 nm in this scheme, a potential 5-bit resolution can be realized with an additional spectral compression module.[16,24] In previous 5-bit schemes, 32 TDLs are required for coding synchronization. The novel scheme utilizing an LCFBG rather than multiple TDL can efficiently reduce the structure complexity and cost in practical applications, which conforms to the trend of integration and miniaturization of all-optical ADC.

References

[1] Walden R H 1999 *IEEE J. Sel. Areas Commun.* **17** 539
[2] Valley G C 2007 *Opt. Express* **15** 1955
[3] Shoop B L 2001 *Photonic Analog-to-Digital Conversion* (Berlin: Springer-Verlag)
[4] Juodawlkis P W 2001 *IEEE Trans. Microw. Theory Technol.* **49** 1840
[5] Ho P P, Wang Q Z and Chen J 1997 *Appl. Opt.* **36** 3425
[6] Konishi T, Tanimura K and Asano K 2002 *J. Opt. Soc. Am. B* **19** 2817
[7] Kang Z, Yuan J H, Li S, Xie S L, Yan B B, Sang X Z and Yu C X 2013 *Chin. Phys. B* **22** 114211
[8] Oda S I, Maruta A and Kitavama L I 2004 *IEEE Photon. Technol. Lett.* **16** 587
[9] Oda S I and Maruta A 2005 *IEEE Photon. Technol. Lett.* **17** 465
[10] Oda S I and Maruta A 2005 *IEEE Trans. Commun.* **E88-B** 1963
[11] Goto H, Konishi T and Nishitani T 2008 *The* 10*th Anniversary International Conference on Transparent Optical Networks*, June 22–26, 2008, Athens, Greece, p. 124
[12] Nishitani T, Konishi T and Itoh K 2007 *Opt. Express* **15** 15812
[13] Nishitani T, Konishi T and Itoh K 2007 *Opt. Express* **15** 17025
[14] Nishitani T, Konishi T and Itoh K 2008 *IEEE J. Selec. Top. Quantum Electron.* **14** 724
[15] Nishitani T, Konishi T and Itoh K 2007, 33*rd European Conference and Ehxibition of Optical Communication*, September 16–20, 2007, Berlin, Germany, p. 1
[16] Konishi T, Takahashi K, Matsui H, Satoh T and Itoh K 2011 *Opt. Express* **19** 16106
[17] Yuan J H, Sang X Z, Yu C X, Zhou G Y and Hou L T 2010 *Chin. Phys. B* **19** 074218
[18] Liang R 2011 "All-optical Quantization Based on the Raman Self-frequency Shift and Spectral Compression", Ph. D. dissertation (Chengdu: University of Electronic Science and Technology of China)
[19] Othonos A 1997 *Rev. Sci. Instrum.* **68** 4309
[20] Sun Y, Yun C, Lin J, Qian Y, Bai B, Yang Y and Qiu W 1999 *J. Optoelectron. Laser* **10** 228
[21] Naguib I I, Moustafa H A and Okaz M A 2008 25*th National Radio Science Conference,* March 18–20, 2008, Tanta, Egypt, p. 1
[22] Yu Z H 2006 "Researches on Theory and Applications of Fiber Gratings", Ph. D. dissertation (Beijing: Beijing University of Posts and Telecommunications)
[23] Yamada M and Sakuda K 1987 *Appl. Opt.* **26** 3474
[24] Kang Z, Yuan J H, Wu Q, Wang T, Li S, Sang X Z, Yu C X and Farrell G 2013 *IEEE Photon. J.* **5**7 201109